

The Impact of Amazonian Deforestation on Dry Season Rainfall

ANDREW J. NEGRI AND ROBERT F. ADLER

Laboratory for Atmospheres, NASA Goddard Space Flight Center, Greenbelt, Maryland

LIMING XU*

Department of Hydrology and Water Resources, The University of Arizona, Tucson, Arizona

JASON SURRATT

Department of Marine, Earth and Atmospheric Sciences, North Carolina State University at Raleigh, Raleigh, North Carolina

(Manuscript received 31 December 2002, in final form 10 October 2003)

ABSTRACT

Many modeling studies have concluded that widespread deforestation of Amazonia would lead to decreased rainfall. Geosynchronous visible and infrared satellite data over southwest Brazil are analyzed with respect to percent cloudiness, and rain estimates are analyzed from both the Tropical Rainfall Measuring Mission and Special Sensor Microwave Imager. The studies conclude that in the dry season, when the effects of the surface are not overwhelmed by synoptic-scale weather disturbances, shallow cumulus cloudiness, deep convective cloudiness, and rainfall occurrence all are larger over the deforested and nonforested (savanna) regions than over areas of dense forest. This paper speculates that this difference is in response to a local circulation initiated by the differential heating of the region's varying forestation. Analysis of the diurnal cycle of cloudiness reveals a shift in the onset of convection toward afternoon hours in the deforested and toward the morning hours in the savanna regions when compared to the neighboring forested regions. Analysis of 14 years of monthly estimates from the Special Sensor Microwave Imager data revealed that in August there was a pattern of higher monthly rainfall amounts over the deforested region. Analysis of available rain gauge data showed an increase in regional rainfall since deforestation began around 1978.

1. Introduction

Initial modeling efforts assessing the impact of Amazonian deforestation assumed widespread deforestation. Nobre et al. (1991) ran simulations using a global spectral model and found that large-scale conversion of forest to pasture decreased the precipitation by 25%. Using the Goddard Global Circulation Model (GCM), Walker et al. (1995) ran a 5-day simulation and showed a decrease in precipitation of 8% in the wettest month of the year. The National Center for Atmospheric Research (NCAR) community climate model results (Hahmann and Dickinson 1997) noted an eastward shift in wet season precipitation with deforestation rather than an overall decrease over the deforested area. More recent modeling work utilized

a mesoscale model with realistic forcing using a “fish-bone” pattern (Wang et al. 2000). This revealed that mesoscale circulations enhanced cloudiness and localized rainfall as well as dry season enhancement of shallow clouds under weak synoptic forcing. Observations and modeling of landscape heterogeneity resulting from differential land use indicated a direct thermal circulation over areas of the Midwest (Weaver and Avissar 2001).

Observations have not borne out the initial modeling studies. Analysis of outgoing longwave radiation (OLR) from 1974 to 1990 and monthly rainfall at Belem and Manaus both showed upward trends in cloudiness and precipitation, despite deforestation in that period (Chu et al. 1994). Using the Global Historical Climatological Network (GHCN) (Easterling et al. 1996) OLR, and National Centers for Environmental Prediction (NCEP) reanalysis, Chen et al. (2001) noted an increasing trend of precipitation over the Amazon Basin. They found clear evidence in the observed global-scale water vapor convergence patterns that more moisture is moving into the Amazon Basin than in the past. They conclude that this inter-

* Current affiliation: FM Global Research, Norwood, Massachusetts.

Corresponding author address: Andrew J. Negri, NASA GSFC, Code 912, Greenbelt, MD 20771.
E-mail: negri@agnes.gsfc.nasa.gov

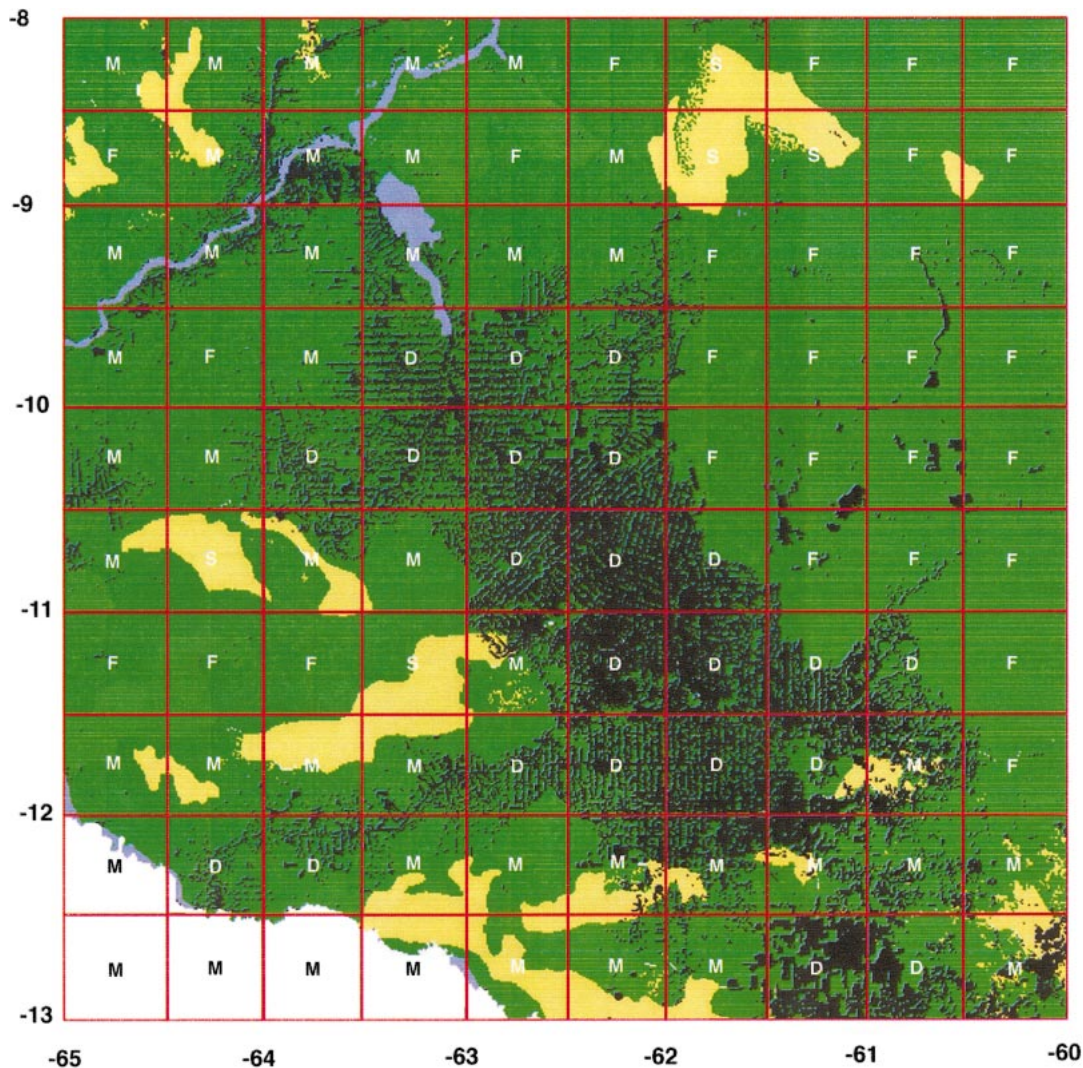


FIG. 1. Land surface classification from Landsat data over a heavily deforested region of Rondonia, Brazil. Classification of 0.5° grid boxes is **F** (forested), **D** (deforested), **S** (savanna), and **M** (mixed).

decadal change in the global divergent circulation has suppressed the full impact of deforestation. When the dry season in particular was examined, higher temperatures, higher sensible heat flux, and deeper convective boundary layers over the deforestation were found (Gash and Nobre 1997). Using Geostationary Operational Environmental Satellite visible imagery, an enhanced frequency of shallow cumulus cloud where forest was cleared was observed (Cutrim et al. 1995). Calvert et al. (1997) observed increased surface temperature in deforested regions. Surface effects have also been linked to urban areas. For example, Tropical Rainfall Measuring Mission (TRMM) data have revealed an average rain-rate increase of 28% downwind of urban areas (Shepherd et al. 2002),

also the likely result of land-use-induced mesoscale circulations.

The meteorology of the state of Rondonia in southwest Brazil has been examined in great detail during the Large-Scale Biosphere Wet Season Campaign (LBA/WETAMC). An overview of that experiment is given by Silva Dias et al. (2002), who also present a brief summary of the available literature on the effects of deforestation upon rainfall. Anagnostou and Morales (2002) examined wet season rainfall using both in situ National Aeronautics and Space Administration Tropical Ocean Global Atmosphere (NASA TOGA) radar data and TRMM rainfall estimates. Betts and Jakob (2002) compared model forecasts to observations of the diurnal cycle during WETAMC,

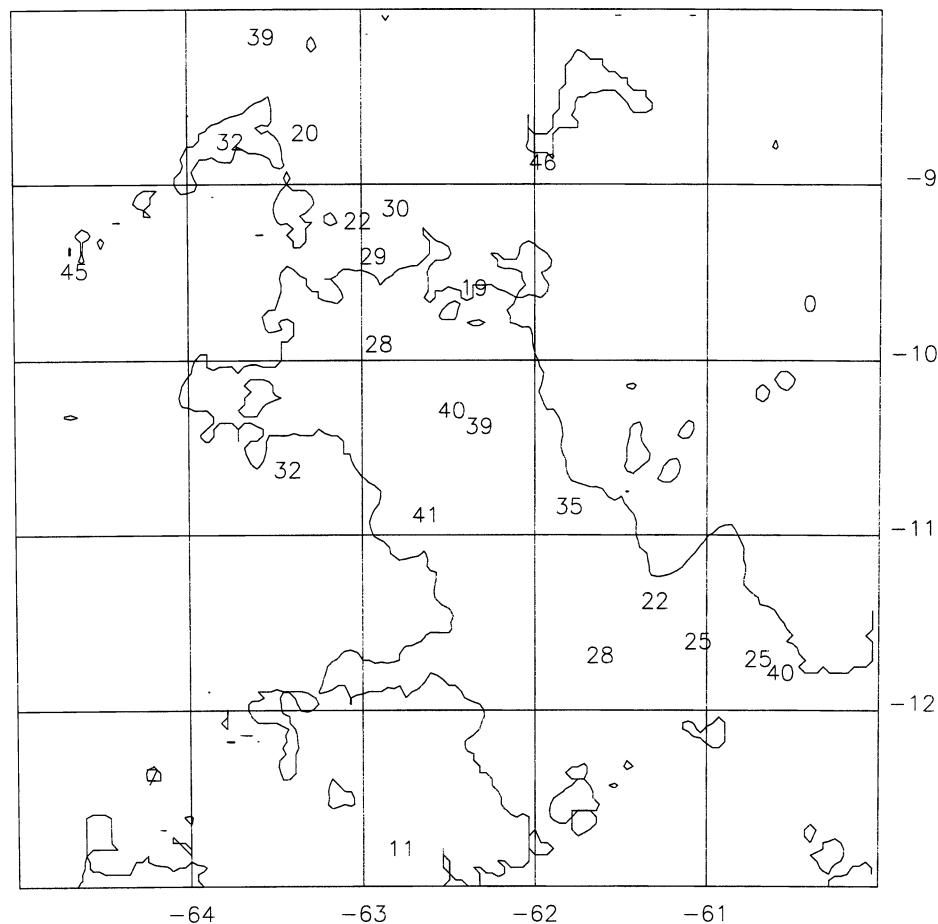


FIG. 2. Mean (1987–96) August rainfall from the Global Historical Climatological Network of gauges. The outline of the deforestation is superimposed.

as did Machado et al. (2002) using geosynchronous satellite-derived cloud amount and in situ radar data. Negri et al. (2002a) used TOGA radar data as verification of the diurnal cycle of satellite-based rain estimates over much of northern South America. A Dry-to-Wet Atmospheric Mesoscale Campaign was conducted in the region during September–November 2002. Durieux et al. (2003) examined the impact of deforestation on cloud cover and precipitation, and in section 4 we compare their results to ours.

The objectives of this study are to demonstrate that, observationally, differences in cloud cover and rainfall exist between regions of forest and pasture. We speculate that, in the dry season, increased surface heating over deforested regions creates a direct thermal circulation, which increases the occurrence of shallow cumulus clouds, deep convective cloudiness, and rainfall. Similar (and more pronounced) effects are noted over a small, naturally unforested region of savanna, suggesting that size or scale may play a role in modulating the resultant circulation. For example

the models using total deforestation of the Amazon may be correct but, in fact, the deforestation has occurred on scales much smaller and more spatially complex.

2. Data

This study relies primarily on data from the Geostationary Operational Environmental Satellite (GOES). It utilizes 10.7- μm infrared (IR) cloud data for the analysis of deep convection and 0.6- μm visible (VIS) data for shallow cumulus clouds. Landsat data are used to identify regions of deforestation. Figure 1 shows the Landsat-derived surface classification [Instituto Nacional de Pesquisas Espaciais/Centro de Previsão de Tempo e Estudos Climáticos (INPE/CPTEC) data adapted from INPE/CPTEC Web site: <http://lba.cptec.inpe.br/lba/indexi.html> courtesy of an anonymous reviewer] for the region of interest, located in southwest Brazil in the state of Rondonia. Darker regions represent deforested areas, while nat-

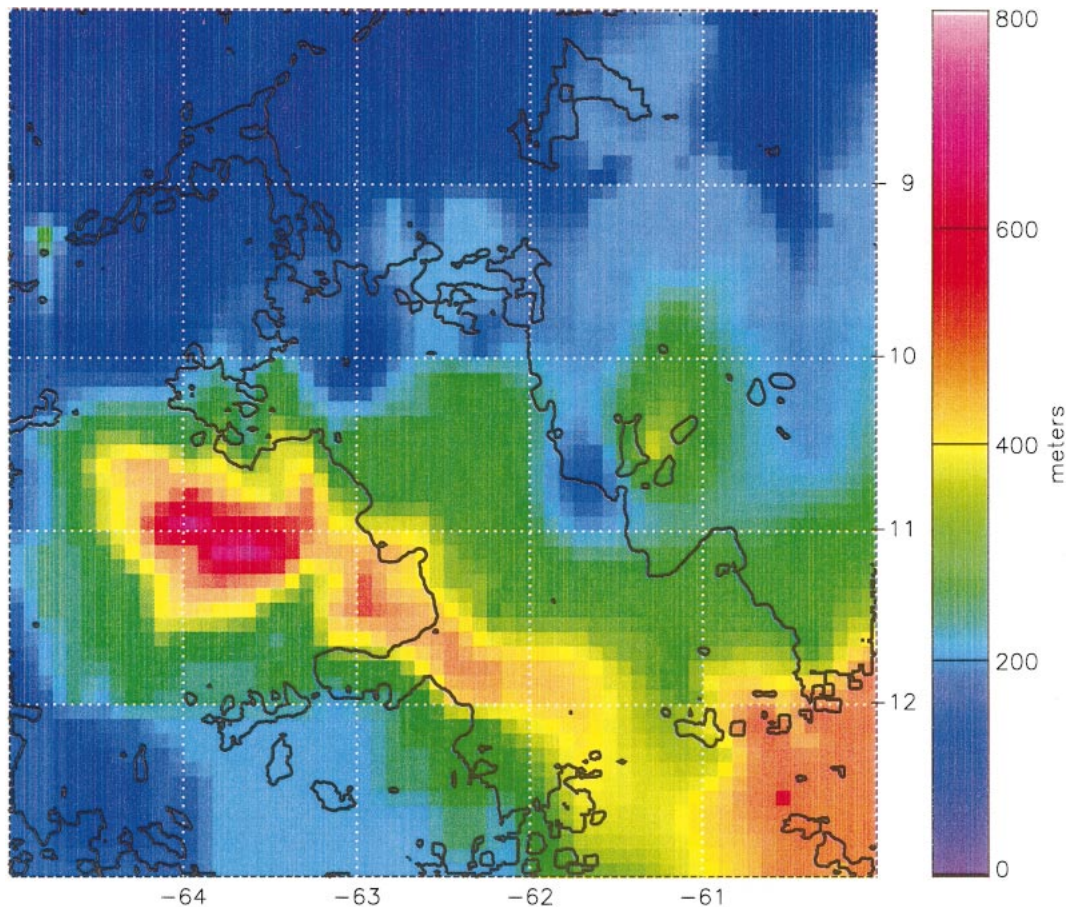


FIG. 3. The topography (m) of the region of interest. The outline of the deforestation is superimposed.

urally occurring savanna is shown in yellow and forested regions in green. We are struck by the similarity of this region and its surroundings to the spatial extent of the Florida peninsula and its juxtaposition between two large bodies of water. We believe that the circulations that arise are similar to peninsula-forced sea-breeze circulations. Deforestation is evident along roads and waterways, and the fish-bone pattern modeled by Wang et al. (2000) is clearly evident. We characterize each 0.5° box for subsequent analysis as deforested (**D**), forested (**F**), mixed (**M**), or savanna (**S**) based on existing land-use climatology from Landsat imagery.

Conventional rain gauge data is sparse in this region. Figure 2 shows the mean (10-yr average) rainfall for August available through the GHCN with the pattern of deforestation from Fig. 1 overlain. Virtually all of the gauges are found within the confines of the deforested region, making a direct, in situ rainfall comparison impossible.

Topography is obviously a concern, as it is not uncommon for mesoscale circulations to develop in re-

sponse to elevated heat sources and mountain/valley geography. Figure 3 shows the topography for this region, lying at the southern extent of the Amazon Basin. The northern portion of the study area is both low (<200 m) and flat. A ridge of higher elevations runs along the western boundary of the deforested area. The maximum elevation is ~ 700 m. While we do not believe that topography plays a major role in initiating circulations in the dry season, its effects cannot be completely discounted. For example, Laurent et al. (2002) found that in the wet season, initiation of mesoscale convective systems was related to relief. We quantify the effect of topography on the diurnal cycle of convection in the next section.

Microwave data were available from two sources, the TRMM Microwave Imager (TMI) for the period January 1998 to the present and data from the Special Sensor Microwave Imager (SSM/I) dating back to July 1987. Microwave radiances from both instruments were processed through the Goddard Profiling (GPROF) algorithm (Kummerow and Giglio 1994;

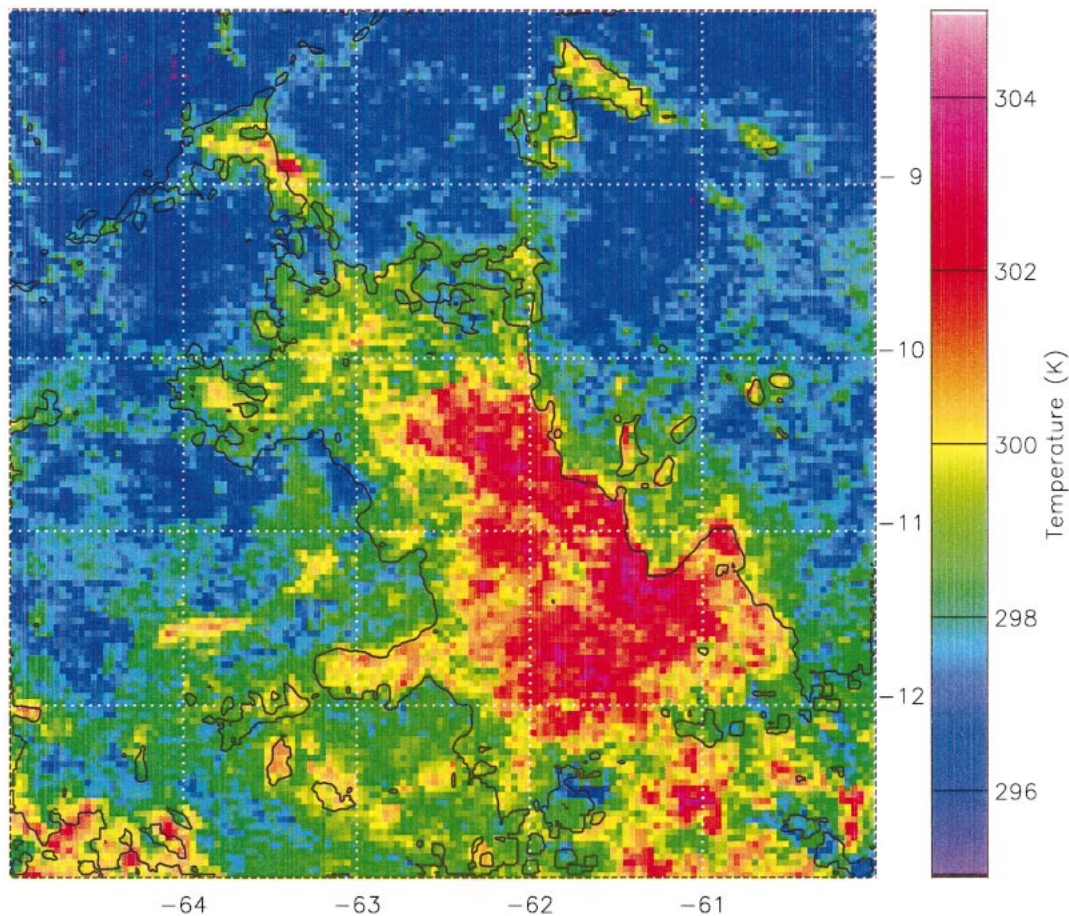


FIG. 4. GOES 4-km infrared composite mean (clear sky) temperatures at 1230 LT for Aug 2000. The outline of the deforestation is superimposed.

Kummerow et al. 2000) to produce monthly surface rainfall (SSM/I) and rain occurrence (TMI).

3. Results

a. Surface temperature

A composite of GOES infrared-derived surface temperatures (under clear-sky conditions) for 1215 LT¹ during August 2000 (Fig. 4) reveals much about the mean surface conditions of the region. Outlines of the deforestation from Fig. 1 are superimposed. Increased surface heating is evident over the deforested and savanna areas, on the order of 5–10 K, as well as over the urban area of Porto Velho (9°S, 63.5°W). The increased heating is due to the lower specific heat and shorter roughness length of the deforested area. This has also been ob-

served from Geosynchronous Meteorology Satellite (Meteosat) observations (Calvert et al. 1997) and from in situ measurements (Gash and Nobre 1997). The emissivities of bare soil, grassy vegetation, and tree vegetation are comparable (Brutsaert 1982) and account for less than 1.5 K of the observed temperature difference. Cooler temperatures are observed in the higher elevations along the western edge of the deforestation. No cold surges from the south were noted during this period (*Climánlise*, a publication of INPE/CPTEC, available online at <http://www.cptec.inpe.br/products/climanalise/>).

b. Visible-channel cumulus clouds

A 10-day period of suppressed conditions enabled us to examine the effect of the contrasting surface conditions on low-level cumulus formation. The percent occurrence of cumulus cloudiness in the GOES visible

¹ GOES-East begins scanning at 15 and 45 min past the hour, and scans the study area about 15 min later. The study area is 4 h earlier than UTC.

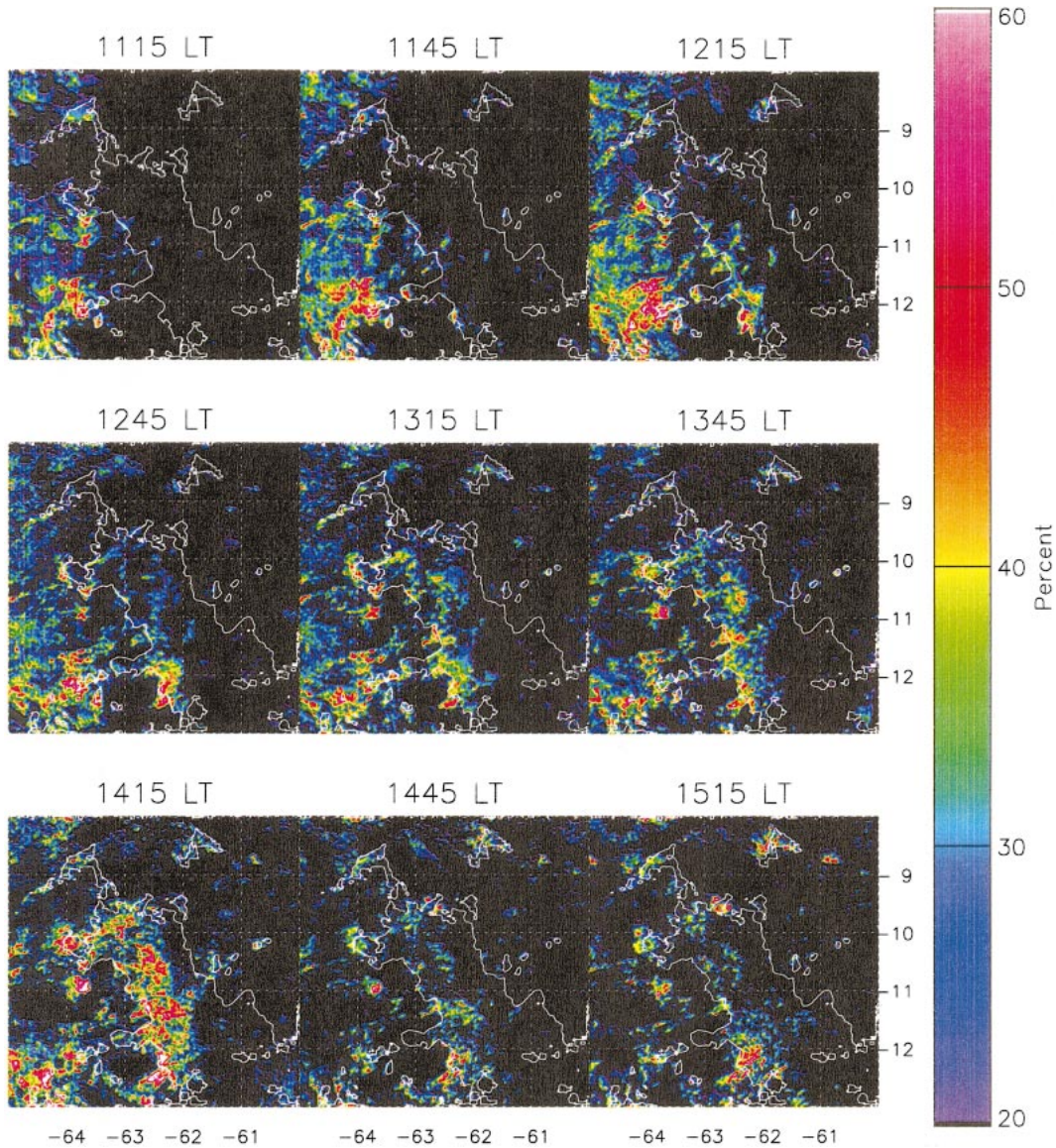


FIG. 5. Percent occurrence of cumulus cloudiness in the GOES visible channel for the period 1115–1515 LT 10–20 Aug 2001. The outline of the deforestation is superimposed.

channel² for the period 1115–1515 LT 10–20 August 2001 is shown in Fig. 5. The outline of the deforestation is superimposed. Preexisting cumulus is already apparent to the west of the deforested region at 1115 LT. Convection develops within the deforested area by 1215, reaching an areal maximum at 1415. Under prevailing low-level easterly flow, we would expect the convergence and hence cloudiness to maximize on the western (upslope) portion, as observed. The dynamic range of the visible sensor on *GOES-8* has declined

² The visible pixel must be in the top 20% brightest pixels for the scene, and have an IR temperature colder than 300 K.

consistently since launch, complicating the quantitative use of this data.

c. Deep convective cloudiness

The occurrence of deep convection can be represented by the fractional occurrence of cloud colder than 225 K. (This threshold is arbitrary, and results are similar if 255 K is chosen.) Figures 6 and 7 display the fractional coverage of cold cloud as measured by the GOES IR sensor for August 2000/01 and September 2000/01, respectively. To ensure frequent and consistent sampling, the 30-min interval GOES data has been

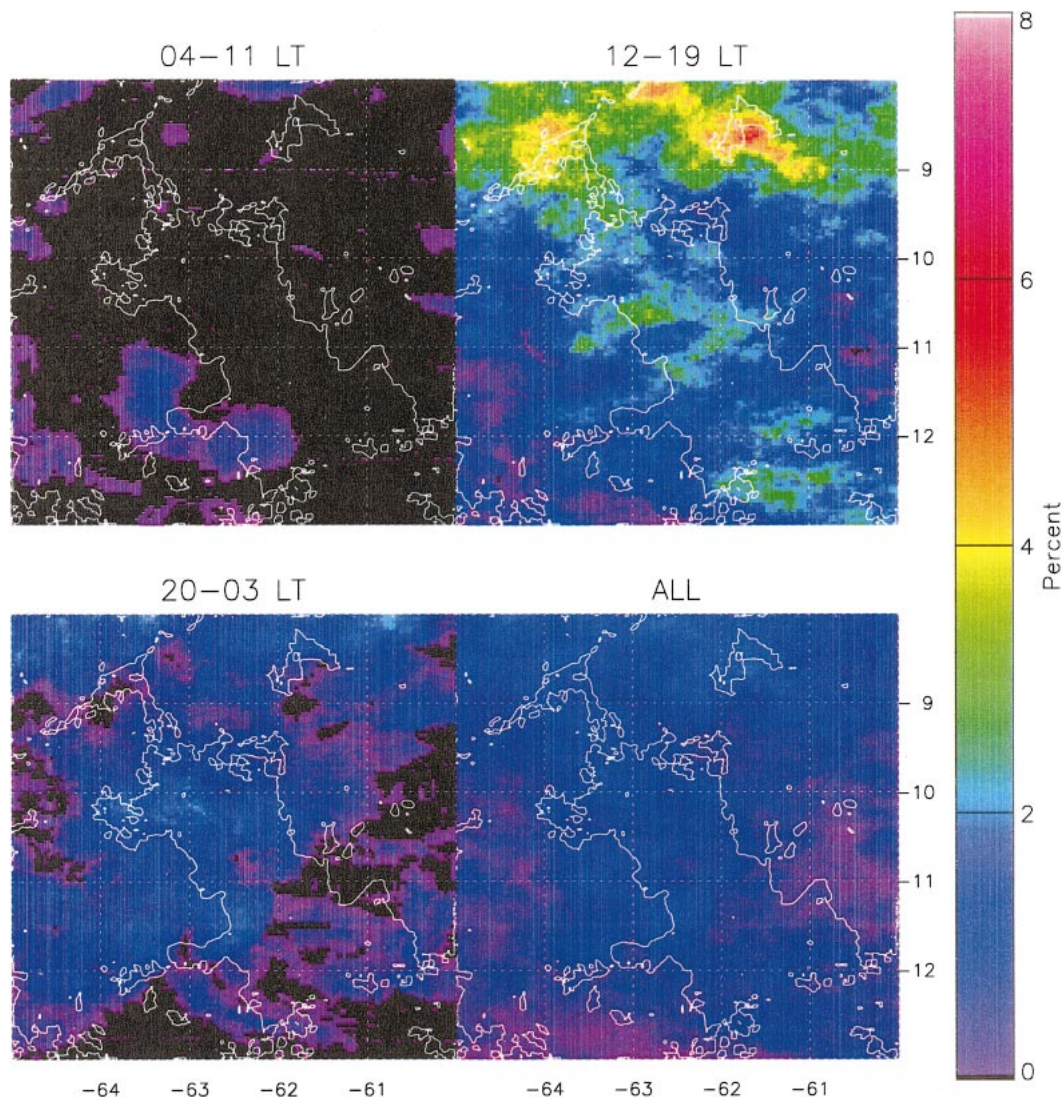


FIG. 6. Percent occurrence of cold (225 K) cloudiness from GOES 4-km infrared data for Aug 2000/01. Half-hourly GOES data have been composited into three 8-h periods and a daily total.

accumulated into three 8-h periods, plus the daily total (bottom-right panel). This stratification was done to enable us to compare with the more limited TRMM rainfall sampling presented in the next section. The impact of deforestation on the cloud amount is most pronounced in August in the period 1200–1900 LT. Note the increased frequency of cold cloud within the confines of the deforestation. Interestingly, two other areas to the north of the main area of deforestation also appear to spawn frequent convection. One area is the inverted V-shaped savanna region identified in Fig. 1. The other is a region of deforestation associated with the urban area of Port Velho. These two areas spawn convection at twice the frequency of the larger deforested region. In September, the aforementioned two

areas are also active regions of convection (almost 20% of the time period 1200–1900 LT). The effects of the main deforestation area are apparent in the increased cloud cover at both 1200–1900 and 2000–0300 LT in both August and September. The effect of a strong meridional gradient in precipitation (and presumably cold cloud) across this region complicate these findings.

It is hypothesized that the differential heating across these regions of deforestation and naturally occurring savanna creates a local, direct circulation, which increases the cloudiness over these regions. We examined all months, but found these effects only in August (the drier month) and September (the onset of the wet season), when the effects of the surface are not over-

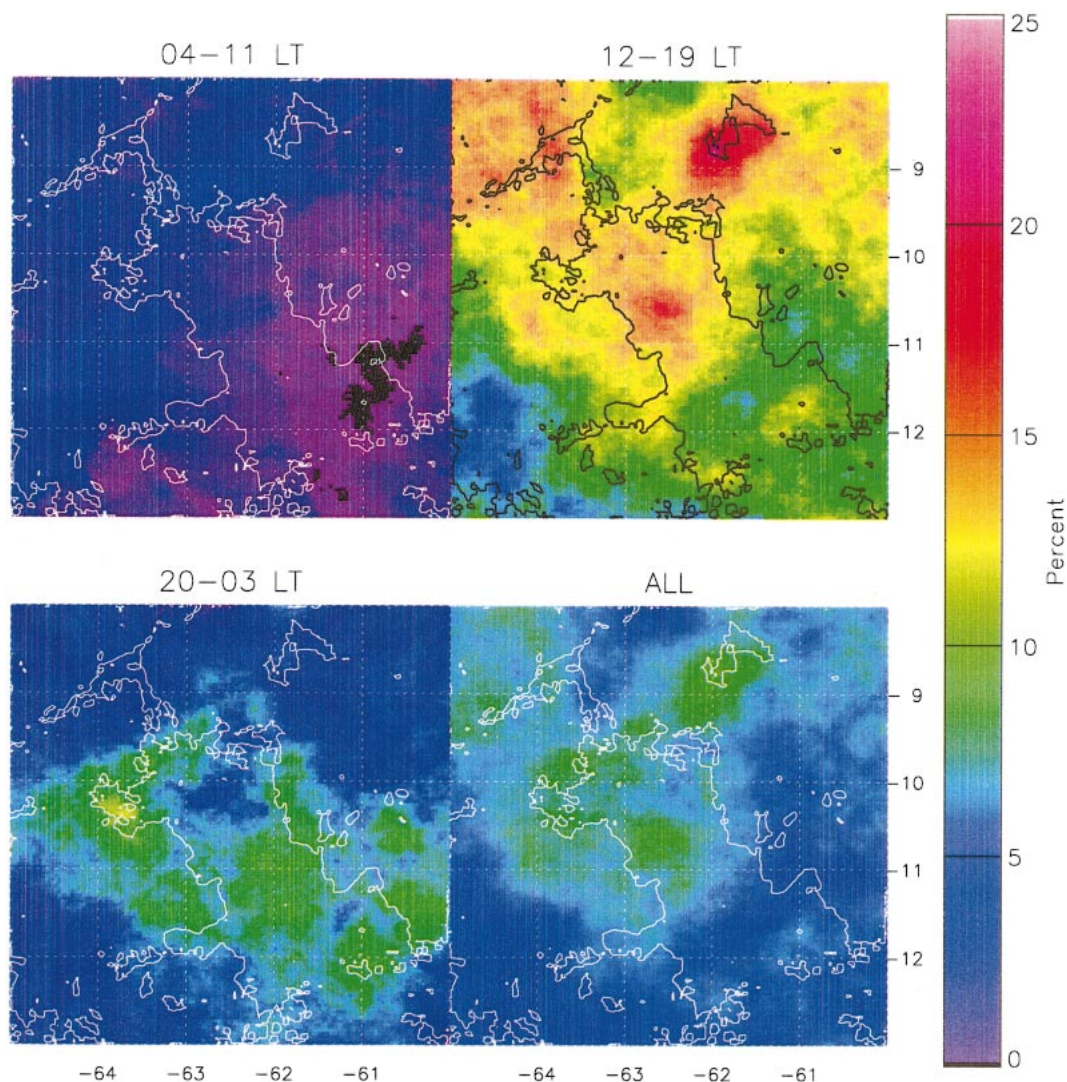


FIG. 7. As in Fig. 6 except Sep 2000/01.

whelmed by the transport of synoptic-scale moisture into the region.

To accumulate enough sampling at 30-min resolution to adequately describe the diurnal cycle, we combine the cloudiness data for the four months of August and September 2000/01. Figure 8 displays a time series of the mean IR cloudiness (225-K threshold) for the various surface types, as characterized by the Landsat data. The surface type with the highest amplitude diurnal signal is the savanna, peaking at 1530 LT. Of interest is the difference between the diurnal signals for the forested (green) and deforested (red) curves. The percent cold cloudiness is slightly higher in the forested regions from 0300 until 1530 after which the deforested regions have a higher per-

cent cloudiness. Times at which the difference in these means is significant at the 0.05 (or less) level are indicated by an "S" along the top. Mean percentages (averaged throughout the diurnal cycle) show no significant difference between the deforested (2.90%), forested (2.92%), or mixed (2.90%) boxes. Rather, we detect a shift in the diurnal cycle towards the afternoon hours over the deforested region. Interestingly, the development of convection over the savanna begins a few hours earlier than the other surface types. A shift in the diurnal cycle due to urban effects in the Houston, Texas, area was found by Shepherd and Burian (2003).

A word about topography: the region is at the southern extent of the Amazon Basin. While the northern portion of the region is flat and under 100 m in ele-

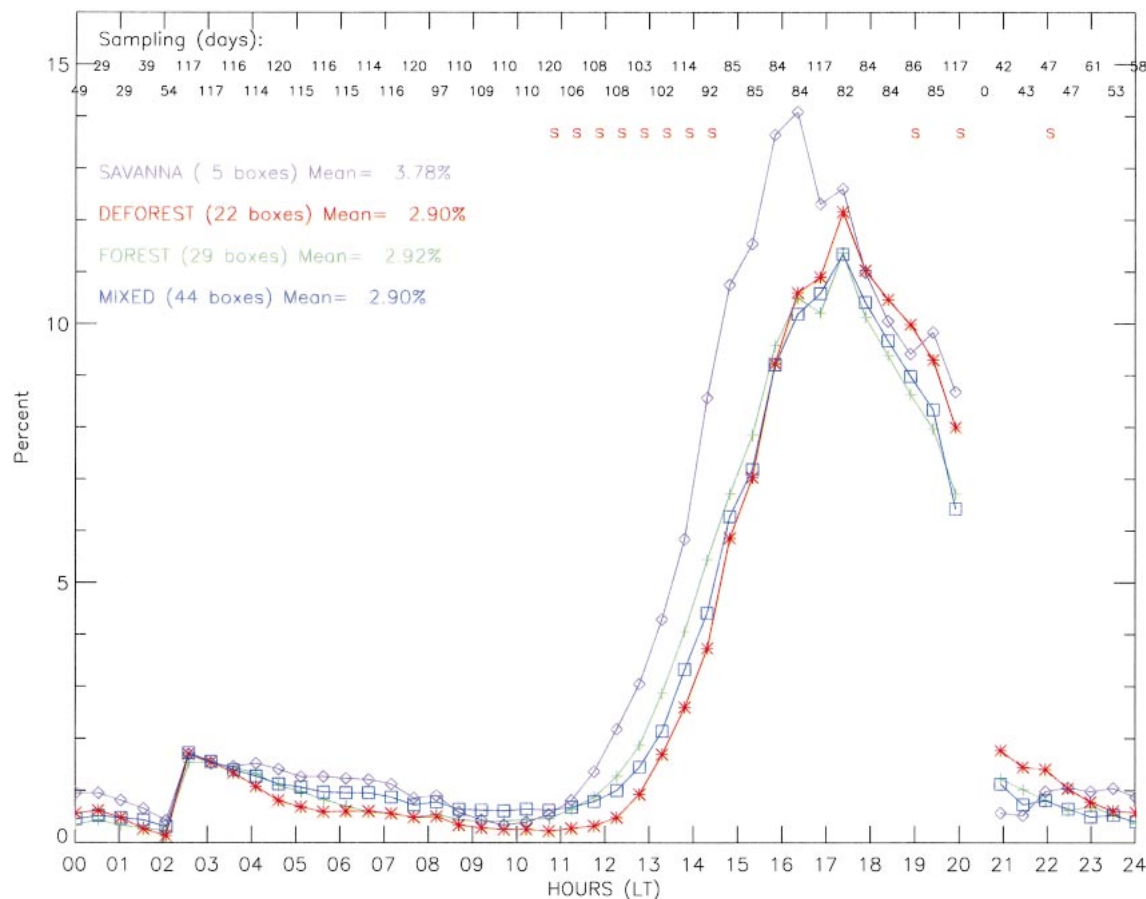


FIG. 8. Time series of the mean percent cloudiness data for Aug–Sep 2000/01 stratified into the four indicated surface types. The significance (<0.05) of the t test for the difference in the mean percent cloudiness between the forested and deforested points is denoted by an “S” plotted across the top. Sampling (maximum of 122 days) is plotted along the top.

vation, there is a ridge of higher land (300–700 m) that runs WNW to SSE across the southern portion of the area. An analysis of the effect of topography on cloud amount is shown in Fig. 9, the diurnal cycle of cold cloudiness, stratified by elevation. Because the region experiences a north–south gradient in cloudiness with lower elevations to the north, we do not see increases in cloudiness with elevation as we might expect. In fact, the opposite effect is seen. The peak of the diurnal cycle of cloudiness is the same at all elevations, namely 1700 LT.

d. Rainfall occurrence

Data from the TRMM were analyzed for the percent occurrence of rain for the periods matching the IR data in Figs. 6 and 7. TRMM is in a 35° inclination orbit and precesses through the diurnal cycle every

46 days.³ Rain rates are produced by the application of the Goddard profiling (GPROF) algorithm (Kummerow and Giglio 1994; Kummerow et al. 2000) to 0.1° -resolution data from the TMI. Results for the occurrence of rainfall (0.1 mm h^{-1} instantaneous threshold) are shown in Figs. 10 and 11. Results for August 2000/01 (Fig. 10) confirm the IR results of Fig. 6; that is, increased occurrence of rainfall over the savanna, over the deforested strip to the west, and over the center of the main area of deforestation, in the period 1200–1900 LT. Results for September (Fig. 11) indicate an increased probability of rain over the deforestation during the period 2000–0300 LT. The preferred region of rainfall occurrence is just southwest of the savanna during the period 1200–1900 LT. Qualitatively, the comparison of TRMM-derived per-

³ A note on sampling: the TMI, with observations aggregated over an 8-h period, will sample a two-month period about 15–25 times [see Negri et al. (2002b) for more on TRMM sampling].

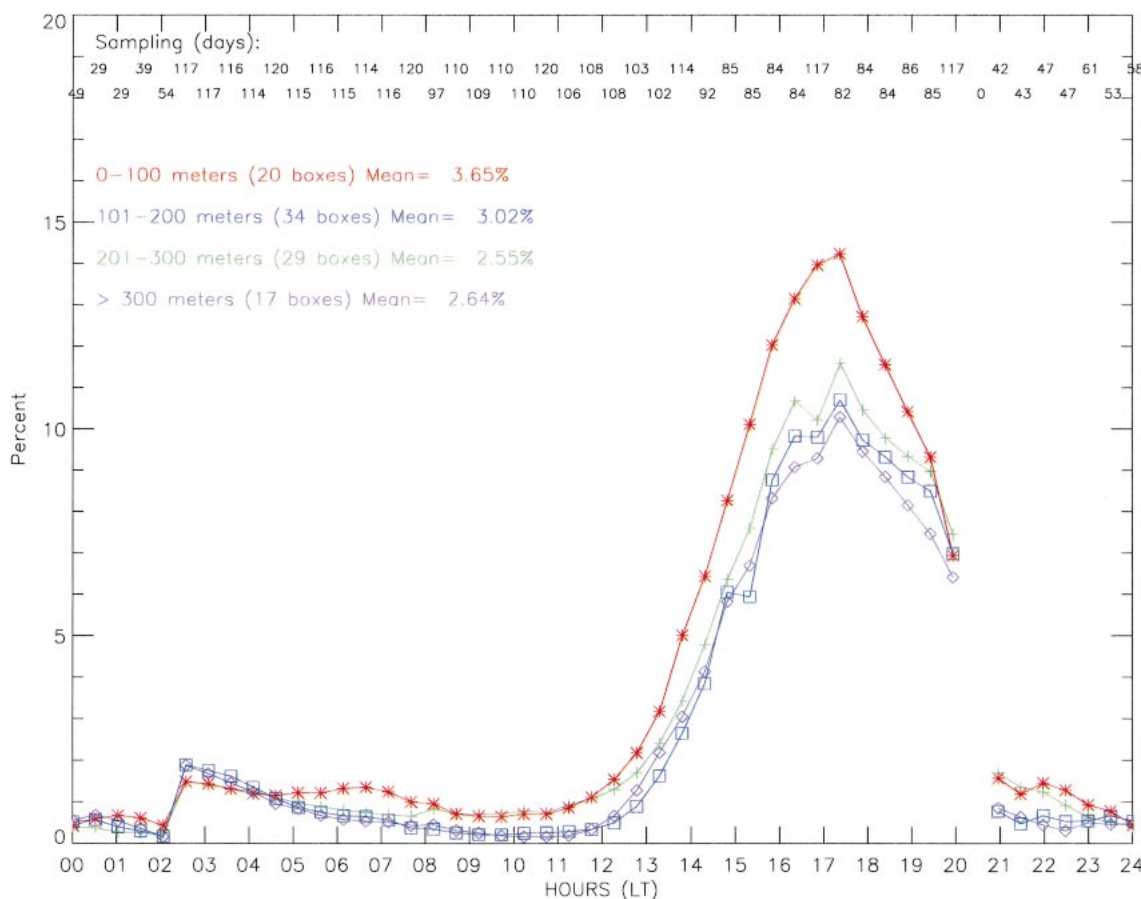


FIG. 9. As in Fig. 8 except stratified by elevation.

cent rain and GOES-derived percent cloud seems to match up better in August than September. We suspect that the much lower sampling of the TRMM and the imperfect relationship between cold cloudiness and rainfall may account for some of this mismatch.

e. Rain rate

A longer record of data is available from the Special Sensor Microwave Imager, a series of sun-synchronous satellites that have overpasses at 0600/1800 LT. The SSM/I provides about 40 samples month⁻¹ over this region. The results of the mean GPROF-derived rain rate at 0.5° resolution for the 14-yr period of record (Fig. 12) revealed that in August (top) the mean rain rate did show a distinct increase over the center of the deforested area. The effect of deforestation during the other months was not as obvious as in, for example, September (Fig. 12, bottom). During the wet season moisture is abundant, negating the effects of the surface, while at the onset of the dry season moisture is limited, inhibiting convection. Results comparing the difference between the afternoon and morning overpasses were

similar due to the lack of rainfall at the 0600 LT overpass time.

f. Long-term trends

Figure 13 shows the analysis of gauge measured rainfall by Webber and Willmott (1998) for August 1960–78 (predeforestation, top) and August 1979–90 (postdeforestation, bottom). Mean areal rainfall has increased by 13%, from 34.7 to 39.1 mm, notably in the north and west. It is unclear how many gauges have been used to construct this analysis and how many rain events it represents. This increasing trend has been noted over the Amazon by Chen et al. (2001).

4. Conclusions

We have analyzed geosynchronous (GOES) infrared satellite data with respect to cloudiness and have analyzed passive microwave data from sensors aboard the Tropical Rainfall Measuring Mission satellite with respect to rainfall occurrence. We conclude that in the dry season (August), when the effects of the surface

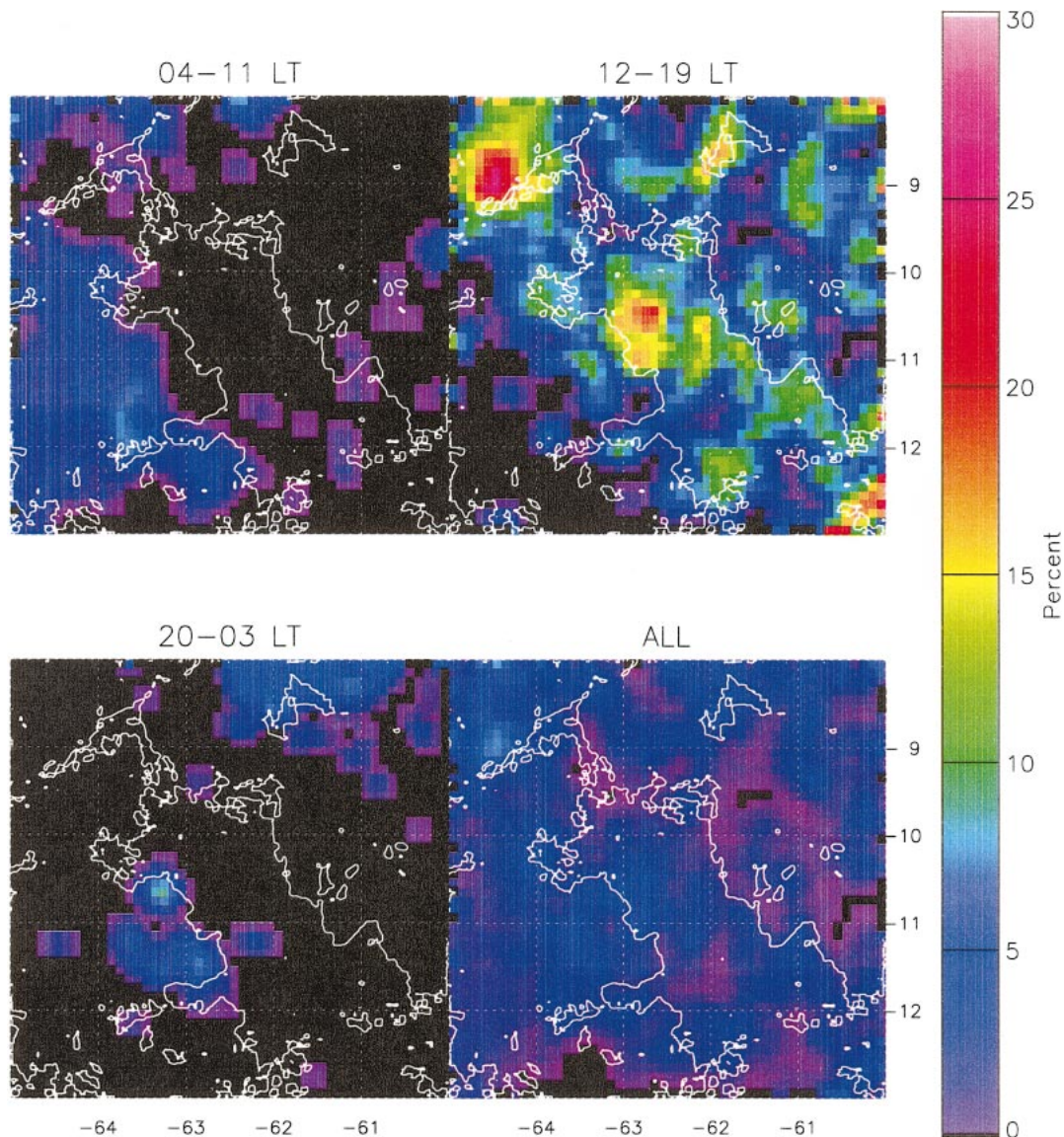


FIG. 10. Percent occurrence of rain at 0.1° resolution derived from the application of the GPROF algorithm to data from the TRMM Microwave Imager for Aug 2000/01. Data have been composited as in Fig. 6.

are not overwhelmed by large-scale weather disturbances, the occurrence of cloudiness and rainfall increase over the deforested and nonforested (savanna) regions. During the day, the amount of cloudiness shifts slightly toward afternoon hours in the deforested region as compared to the forested regions. The opposite was true for the naturally occurring savanna, whose diurnal cycle was shifted two hours earlier. Analysis of 14 years of monthly estimates from the Special Sensor Microwave Imager revealed that only in August did the pattern of rainfall show increases over the deforested region.

Analysis of long-term in situ precipitation from the

GHCN is inconclusive, due to both the low rain amounts during this period, and the absence of gauges outside of the deforested regions. Rainfall has increased across the entire region since the onset of deforestation.

The scenario presented here, based on satellite observations of cloudiness and rainfall, is in agreement with the most recent and sophisticated mesoscale models. These conclude that mesoscale circulations induced by a heterogeneous land surface could enhance cloudiness and local rainfall (Wang et al. 2000). The effects are most pronounced in August, during the transition from dry to wet season. It should be

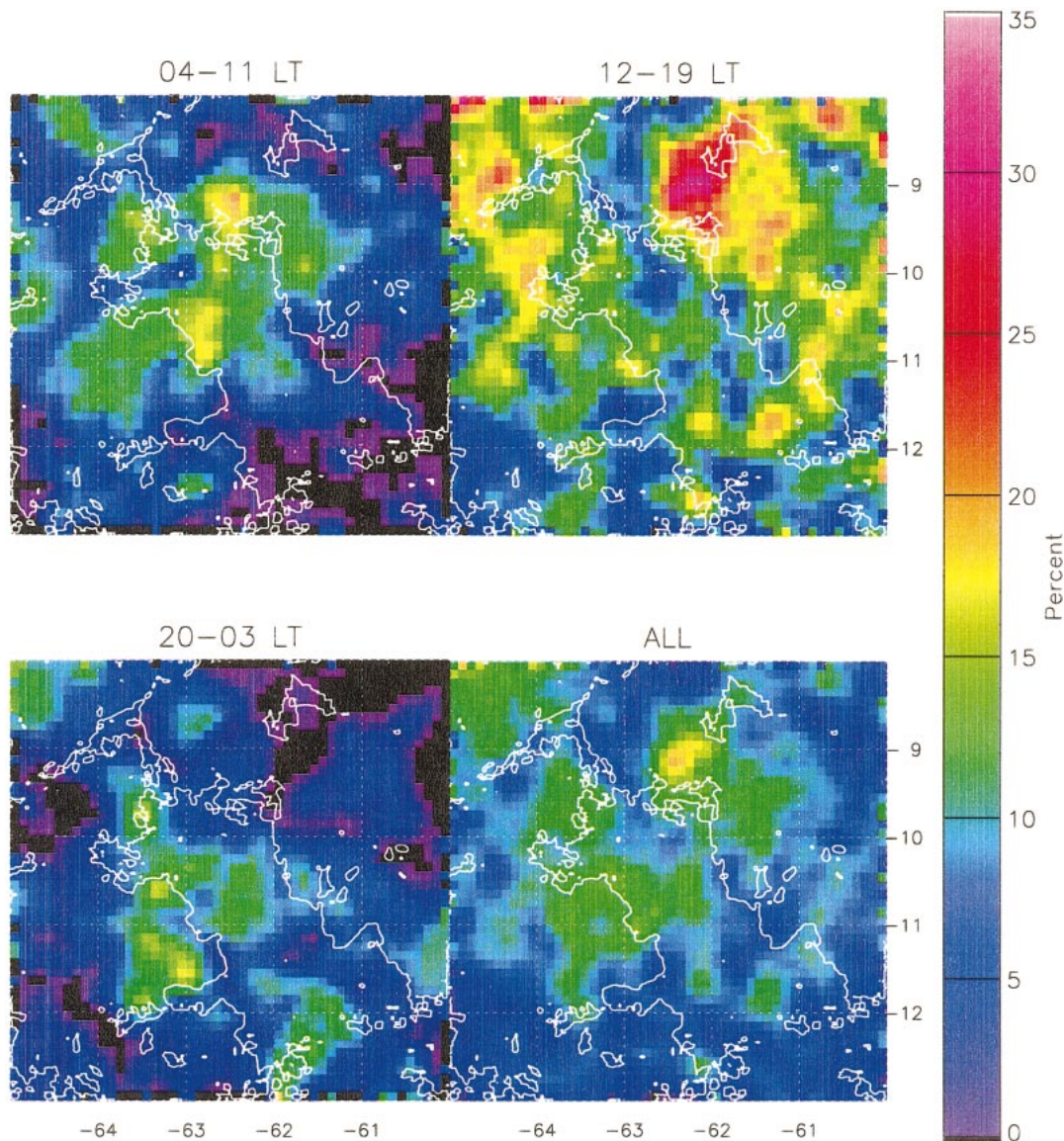


FIG. 11. As in Fig. 9 except for Sep 2000/01.

noted that the effects are rather subtle and appear to be limited to specific time periods (i.e., the dry season). Thus the cumulative effect of this deforestation on annual rainfall and its diurnal cycle is probably small, but requires further study.

Of particular interest was the discovery that the nonforested savanna region apparently exerted a stronger control on the onset of convection than did the larger deforested region. Anthes (1984) hypothesized that planting bands of vegetation with widths on the order of 50–100 km in semiarid regions could result in increases in convective precipitation. Among the mechanisms he proposed was the generation of mesoscale circulations associated with the surface in-

homogeneities created on this scale by the vegetation. It appears as though the contrast in surface cover between the savanna and forested regions is producing this effect, as the horizontal scale of the savanna is ~ 100 km.

In a recent study of the impact of deforestation on cloud cover and precipitation over the Amazon, Durieux et al. (2003) examined 10 years of 3-hourly infrared data from the International Satellite Cloud Climatology Project (ISCCP). The area that they designate as D1 (deforested) is a 2.5° by 2.5° grid cell contained within the area of this study. Durieux found no significant difference in the diurnal cycle of dry season cloud cover between D1 and reference grid cell R1 5° to its north.

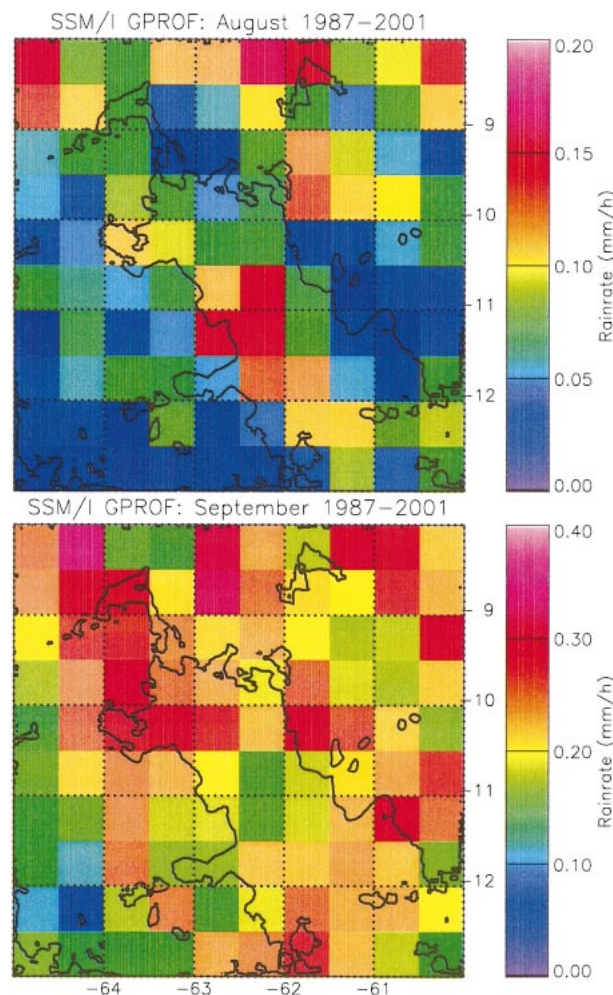


FIG. 12. Mean rain rate 1987–2001 (mm h^{-1}) for (top) Aug, and (bottom) Sep from estimates from the application of the Goddard profiling algorithm to data from the Special Sensor Microwave Imager.

They also found that annually averaged precipitation and high-cloud cover (HCC) were lower in D1 with respect to R1. They attributed this difference not to deforestation but to the sharp meridional gradient in precipitation. These results are in contrast to what we have found in this study, but differences in analysis technique could explain these differences. The grid cell size used by Durieux et al. is certainly a factor, as a 2.5° cell is necessarily more a mixture of surface types than the 0.5° cells in this study. In fact, the difference in forest cover in R1 and D1 is only 7%. We agree with Durieux et al. that the sharp meridional gradient in precipitation could complicate the effect of deforestation, particularly in the dry season.

The effects described here are small and have only been observed in the dry season, so the consequences for climate change are likely to be small. Numerical models are the logical platform for investigating the linkage between the deforested land surface and the

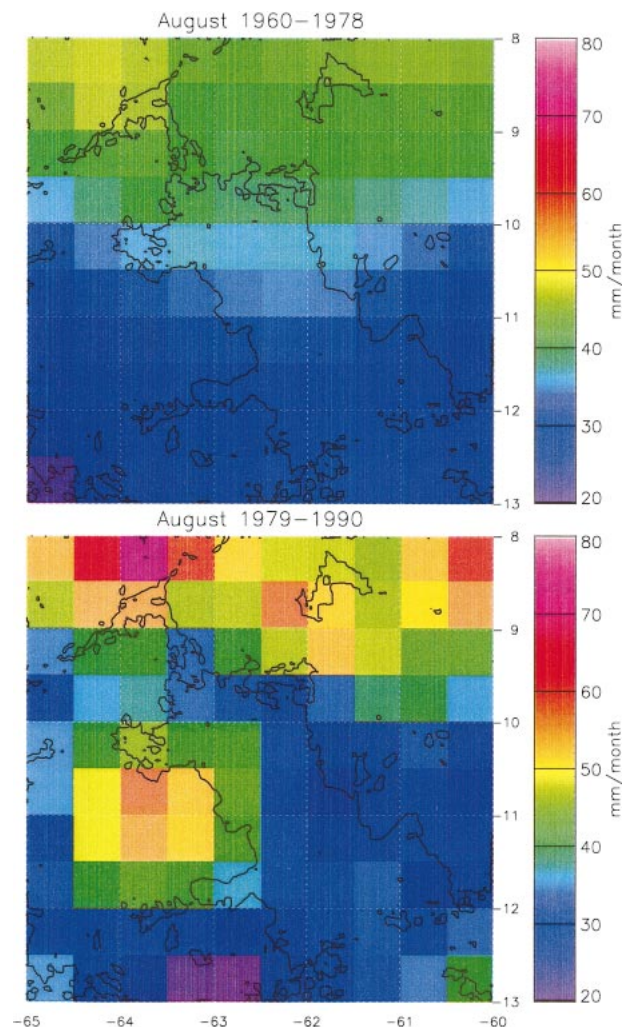


FIG. 13. Mean rainfall (mm month^{-1}) for (top) Aug 1960–78 and (bottom) Aug 1979–90.

cloud–precipitation components of the water cycle, and that is an area of future research.

Acknowledgments. The authors acknowledge the support of NASA's Atmospheric Dynamics and Remote Sensing Program, Dr. Ramesh Kakar, Manager. We acknowledge the University of New Hampshire, EOS-WEBSTER Earth Science Information Partner (ESIP) as the data distributor for the rain gauge analysis. The comments of an anonymous reviewer were greatly appreciated.

REFERENCES

- Anagnostou, E. N., and C. A. Morales, 2002: Rainfall estimation from TOGA observations during LBA field campaign. *J. Geophys. Res.*, **107**, 8068, doi:10.1029/2001JD000377.
- Anthes, R. A., 1984: Enhancement of convective precipitation by mesoscale variations in vegetative covering in semiarid regions. *J. Climate Appl. Meteor.*, **23**, 541–554.

- Betts, A. K., and C. Jakob, 2002: Evaluation of the diurnal cycle of precipitation, surface thermodynamics and surface fluxes in the ECMWF model using LBA data. *J. Geophys. Res.*, **107**, 8045, doi:10.1029/2001JD000427.
- Brutsaert, W. H., 1982: *Evaporation into the Atmosphere*. D. Reidel, 299 pp.
- Calvert, J.-C., R. Santos-Alvala, G. Jaubert, C. Delire, C. Nobre, I. Wright, and J. Noilhan, 1997: Mapping surface parameters for mesoscale modeling in forested and deforested southwestern Amazonia. *Bull. Amer. Meteor. Soc.*, **78**, 413–423.
- Chen, T.-C., J.-H. Yoon, K. J. St. Croix, and E. S. Takle, 2001: Suppressing impacts of the Amazonian deforestation by the global circulation change. *Bull. Amer. Meteor. Soc.*, **82**, 2209–2216.
- Chu, P.-S., Z.-P. Yu, and S. Hastenrath, 1994: Detecting climate change concurrent with deforestation in the Amazon Basin: Which way has it gone? *Bull. Amer. Meteor. Soc.*, **75**, 579–582.
- Cutrim, E., D. W. Martin, and R. Rabin, 1995: Enhancement of cumulus clouds over deforested lands in Amazonia. *Bull. Amer. Meteor. Soc.*, **76**, 1801–1805.
- Durieux, L., L. A. T. Machado, and H. Laurent, 2003: The impact of deforestation on cloud cover over the Amazon arc of deforestation. *Remote Sens. Environ.*, **86**, 132–140.
- Easterling, D. R., T. C. Peterson, and T. R. Karl, 1996: On the development and use of homogenized climate datasets. *J. Climate*, **9**, 1429–1434.
- Gash, J. H. C., and C. A. Nobre, 1997: Climatic effects of Amazonian deforestation: Some results from ABRACOS. *Bull. Amer. Meteor. Soc.*, **78**, 823–830.
- Hahmann, A. N., and R. E. Dickinson, 1997: RCCM2-BATS model over tropical South America: Applications to tropical deforestation. *J. Climate*, **10**, 1944–1964.
- Kummerow, C. D., and L. Giglio, 1994: A passive microwave technique for estimating rainfall and vertical structure information from space. Part I: Algorithm description. *J. Appl. Meteor.*, **33**, 3–18.
- , and Coauthors, 2000: The status of the Tropical Rainfall Measuring Mission (TRMM) after two years in orbit. *J. Appl. Meteor.*, **39**, 1965–1982.
- Laurent, H., L. A. T. Machado, C. A. Morales, and L. Durieux, 2002: Characteristics of the Amazonian mesoscale convective systems observed from satellite and radar during the WETAMC/LBA experiment. *J. Geophys. Res.*, **107**, 8054, doi:10.1029/2001JD000337.
- Machado, L. A. T., H. Laurent, and A. A. Lima, 2002: Diurnal march of the convection observed during TRMM-WETAMC/LBA. *J. Geophys. Res.*, **107**, 8642, doi:10.1029/2001JD000338.
- Negri, A. J., R. F. Adler, and L. Xu, 2002a: A TRMM-calibrated infrared rainfall algorithm applied over Brazil. *J. Geophys. Res.*, **107**, 8048, doi:10.1029/2001JD000265.
- , T. L. Bell, and L. Xu, 2002b: Sampling of the diurnal cycle using TRMM. *J. Atmos. Oceanic Technol.*, **19**, 1333–1344.
- Nobre, C. A., P. J. Sellers, and J. Shukla, 1991: Amazon deforestation and regional climate change. *J. Climate*, **4**, 957–988.
- Shepherd, J. M., and S. J. Burian, 2003: Detection of urban-induced rainfall anomalies in a major coastal city. *Earth Interactions*, **7**. [Available online at <http://EarthInteractions.org>.]
- , H. Pierce, and A. J. Negri, 2002: Rainfall modification by major urban areas: Observations from spaceborne rain radar on the TRMM satellite. *J. Appl. Meteor.*, **41**, 1853–1865.
- Silva Dias, M. A. F., and Coauthors, 2002: Cloud and rain processes in a biosphere–atmosphere interaction context in the Amazon Region. *J. Geophys. Res.*, **107**, 8072, doi:10.1029/2001JD000335.
- Walker, G. K., Y. C. Sud, and R. Atlas, 1995: Impact of the ongoing Amazonian deforestation on local precipitation: A GCM simulation study. *Bull. Amer. Meteor. Soc.*, **76**, 346–361.
- Wang, J., R. L. Bras, and E. A. B. Eltahir, 2000: The impact of the observed deforestation on the mesoscale distribution of rainfall and clouds in Amazonia. *J. Hydrometeorol.*, **1**, 267–286.
- Weaver, C. P., and R. Avissar, 2001: Atmospheric disturbances caused by human modification of the landscape. *Bull. Amer. Meteor. Soc.*, **82**, 269–281.
- Webber, S. R., and C. J. Willmott, 1998: South American precipitation: 1960–1990 gridded monthly time series (version 1.02). Center for Climatic Research datasets, Dept. of Geography, University of Delaware, 87 pp.